 https://doi.org/10.3311/PPch.18357

Periodica Polytechnica Chemical Engineering, 66(1), pp. 54–69, 2022

Assessment on Performance-properties of Asymmetric Nanofiltration Membranes from Polyethersulfone/n-Methyl-2-pyrrolidone/water Blends with Poly(vinyl pyrrolidone) as Additive

Sabariah Rozali[1], Nurul Hannan Mohd Safari[1], Abdul Rahman Hassan[1,2*], Musa Ahmad[3], Rosli Mohd Yunus[4]

[1] East Coast Environmental Research Institute, Universiti Sultan Zainal Abidin, 21300 Kuala Nerus, Terengganu, Malaysia
[2] Faculty of Innovative Design and Technology, Universiti Sultan Zainal Abidin, 21300 Kuala Nerus, Terengganu, Malaysia
[3] Faculty of Science and Technology, Universiti Sains Islam Malaysia, 71800 Nilai, Negeri Sembilan, Malaysia
[4] Faculty of Chemical and Process Engineering Technology, Universiti Malaysia Pahang, 26600 Pekan, Pahang, Malaysia
* Corresponding author, e-mail: rahmanhassan@unisza.edu.my

Received: 15 April 2021, Accepted: 24 June 2021, Published online: 11 November 2021

Abstract

In this study, the effect of poly(vinyl pyrrolidone) (PVP) additive on the fabrication of asymmetric nanofiltration (NF) membranes was investigated in terms of performance, structural details and key properties. On addition of PVP ranging from 2 to 10 wt% into the dope solution, the fabricated NF membranes exhibited significantly different in properties and improved performance. In particular, the membranes made from 2 wt% PVP had the highest water flux and salt rejection of about 3.61×10^{-6} m^3/m^2s and 44.49 %, respectively. Modeling results revealed that small amount of PVP (2–4 wt%) produced finer structural properties. Moreover, the key properties (r_p, $\Delta x/A_k$ and ζ) of the fabricated NF membranes were found to be within the range of that of commercial NF membranes.

Keywords

poly(vinyl pyrrolidone), nanofiltration, performance-properties, structural details, additive

1 Introduction

Most of the polymeric based asymmetric membranes are prepared by phase inversion process based on immersion precipitation technique [1–6]. During phase inversion process, the formation of ultra-thin skin layer, membrane morphology and pore size characteristic was studied based on flat sheet or single layer asymmetric membranes [7]. Asymmetric membrane has been widely used for gas separation and liquid separation, because the thin top layer plays the role of a selective barrier film, and the porous sub-layer, which includes macrovoids, pores and micropores, offers good mechanical strength [8]. It is well known that the formation of asymmetric membrane depends on kinetic parameters such as exchange rate between solvent and non-solvent, kinetics of phase separation, as well as on thermodynamic parameters such as phase diagrams, polymer/solvent interactions, solvent/non-solvent interactions and interfacial stability. Thus, the materials' selection such as polymers, solvents and non-solvents is very important for fabrication of asymmetric membranes, according to its application [9].

Asymmetric membrane is characterized by a thin and dense skin layer on top of a porous substructure. It is known that the skin layer provides major resistance to the permeation of solute through the membrane, whereas the porous substructure functions exclusively as a mechanical support. The capability of an asymmetric membrane to reject or admit a certain solute species is, therefore, determined by the morphology, pore size and density of the skin layer [10]. In order to control the membrane structure, low molecular weight component or the secondary polymer is frequently used as the additive in the membrane forming system because it offers a convenient and effective way to develop high performance membranes [11].

Additives that has been commonly used in the fabrication of asymmetric polymeric membranes by far can be categorized into:

Cite this article as: Rozali, S., Safari, N. H. M., Hassan, A. R., Ahmad, M., Yunus, R. M. "Assessment on Performance-properties of Asymmetric Nanofiltration Membranes from Polyethersulfone/n-Methyl-2-pyrrolidone/water Blends with Poly(vinyl pyrrolidone) as Additive", Periodica Polytechnica Chemical Engineering, 66(1), pp. 54–69, 2022. https://doi.org/10.3311/PPch.18357

1. polymeric additives such as PVP [12–15] and polyethylene glycol (PEG) [16–18];
2. low molecular weight chemicals, including salts such as lithium chloride (LiCl) [19–21] and lithium perchlorate ($LiClO_4$) [22], inorganic acids (acetic acid, phosphoric acid) [23] and organic acids (propionic acids [24];
3. weak non-solvents such as glycerol [25], and strong non-solvent, water, as an additives in a tiny amount [26]. Nevertheless, the roles of different additives vary in different polymer /solvent/non-solvent systems.

The addition of PVP was found to favor macrovoids formation in the fabrication of asymmetric membranes [12]. The occurrence of macrovoids was associated with the instantaneous demixing mechanism as PVP addition increased the dope's thermodynamic instability in reaction with the non-solvent water. Moreover, the viscosity of the dope solution increased with the amount of the additives, which hindered the diffusions among the components in the phase inversion process (kinetic effect) [27].

During the phase inversion process, it is assumed that the hydrophilic additive (PVP), is dissolved out by water and sites where the PVP exists become micropores. Besides the formation of micropores, it has been generally accepted that the porosity increased and the macrovoids formation disappeared as PVP was added to casting solution [28]. The addition of PVP additives into dope solution can promote the formation of macrovoids in the membranes and pure water flux was thus increased [27, 29].

The low molecular weight PVP tends to form small pores and easily leaches out from the membranes, while most of the high molecular weight PVP remain in the membrane and may block the void interconnection path [30, 31]. It can be concluded that the low rejection and large pore size were due to the larger molecular weight of PEG/PVP tends to form a thicker skin layer containing bigger pores [32]. The presence of a relatively large amount of PVP also resulted in the macropores's suppression [33, 34]. The past studies also recorded the usefulness of PVP as an effective permeation flux promoter, and the thermodynamic effect played a dominant role during the membranes formations [35, 36].

NF membranes were developed recently and had been used for the separation of aqueous solutions containing electrolytes. The combination of steric (sieving) and electrostatic (Donnan) partition effects between membrane and external solutions allowed the NF membrane to be very effective for mixture of organic molecules (neutral or charged) and salts [37, 38]. The possible mechanisms for the separation of electrolytes are:

1. sieving,
2. electrostatic interactions between the membrane and the ions or between the membrane and the ions or between the ions mutually and
3. differences in diffusivity and solubility or a combination of these [37]. Separation of electrolytes ions having different signs and valences can be manipulated according to the rejection differences by the membrane [39].

The transport mechanisms of NF membranes are similar to those of RO and UF membranes which can be described with a phenomenological equation by the irreversible thermodynamic model [40]. Normally, the assumption of this model is that membrane is considered as a black box and no information about the transport mechanism can be obtained from it. Therefore, it is important to determine the structural parameters and the electrostatic properties of NF membranes and to evaluate the transportation mechanisms of NF membranes.

The effects of additives concentration and molecular weight used in dope solution on the performances and properties of polymeric membranes are a very famous and concerned by numerous researchers [41, 42]. However, the relation about the used additives on the structural properties, surface charge and even steric-hindrance factors are neglected. Further analysis and characterization about the mentioned issue are very crucial and vital towards separation and membranes optimizations. Therefore, the main goal of this work is to study the effect of PVP additive on performance-properties which provide an important technical properties and practical knowledge in membranes making and its applications.

1.1 Theoretical background

1.1.1 Irreversible thermodynamics model

The deduction of structural properties of nanofiltration membrane was conducted based on the solution-diffusion mechanism. These involved the use of extended Nernst-Planck equation, Spiegler-Kedem transport equation, SHP model and TMS model [40]. The determination of the membrane parameters that was mentioned above were based on the solution-diffusion mechanism. These involved the using of Spiegler-Kedem transport equation,

SHP model and the combination of the TMS model with the extended Nernst-Plank equation.

The transport phenomena of UF, NF and RO membranes in the pressure-driven process can be described by the irreversible thermodynamics [43, 44]. In general, the transport equations for the components through a NF membrane consist of two components: a diffusion component and a convection component. This is reflected by the transport equation of Spiegler-Kedem [45]:

$$J_s = -P\Delta x\frac{dc}{dx} + (1-\sigma)J_v c. \quad (1)$$

The diffusion component (first term in Eq. (1)) is independent of pressure; the convection term is proportional to the pressure because of Hagen-Poiseuille's law [46]:

$$J_v = \frac{\varepsilon r}{8\eta\tau}\frac{\Delta P}{\Delta x}. \quad (2)$$

At low pressures, both terms contribute to the transport of solutes that through to the membrane. While at higher pressure, the relative importance of convection in the transport will be higher. In the hypothetical case of an infinite pressure, diffusion is negligible compared to the infinite convection flux. Since diffusion of solutes will result in an increase of transport relative to the water transport, the relative transport of solutes is the lowest at infinite pressure. The permeation for component *i* is defined as:

$$R_i = \left(1-\frac{c_{p,i}}{c_{r,i}}\right)\times 100\ \%, \quad (3)$$

and thus, it is maximal at infinite pressure. This value is called the reflection coefficient and appears in Eq. (1) as σ [46].

At non-infinite pressures, Eq. (1) can be solved to calculate the permeation as a function of reflection coefficient and the solute permeability, P_s. The result of this calculation is:

$$R_{\text{real}} = \left(\frac{\sigma(1-F)}{1-\sigma F}\right), \quad (4)$$

with,

$$F = \exp\left(-\frac{1-\sigma}{P}J_v\right). \quad (5)$$

Equation (4) is a well-known Spiegler-Kedem equation. The σ and the P_s can be determined directly from experimental data of the rejection, R_{real} as a function of J_v by a best-fit method. Because Eq. (6) is valid:

$$J_v \to \infty : R_{\text{real}} \to \sigma. \quad (6)$$

The reflection coefficient corresponds to the maximum rejection at an infinitely high permeate volume flux when the filtration flow overtakes solute diffusion. However, the irreversible thermodynamic model is not able to characterize the structural and electrical properties of the membranes because the membrane is assumed to act as a black box containing no description of the molecules transport mechanism.

1.1.2 Steric-Hindrance Pore (SHP) model

An important feature of using the SHP model is to provide a description of the separation properties of developed membranes in terms of two key properties that are pore radius, r_p and ratio of thickness to porosity of the membranes $\Delta x/A_k$. The ion permeation flux inside the membrane can be expressed by the modified Nernst-Planck equation considering the steric-hindrance effects, which is similar to that proposed by past researchers [47–49].

$$J_i = v_i k_i\left[H_{F,iUxC} - H_{D,i}D_i\left(\frac{dc}{dx} + c\frac{ziFd\phi}{RTdx}\right)\right]\ i = 1,2 \quad (7)$$

$H_{D,i}$ and $H_{F,i}$ are called the steric-hindrance parameters related to the wall correction factors of ion *i* under diffusion and convection conditions, respectively, and expressed by the SHP model. Through modifying the pore model, the SHP model can be used to calculate r_p and $\Delta x/A_k$ by the used of single neutral solute [40]. The parameters can be calculated based on the Eqs. (8) and (9):

$$\sigma = 1 - H_F S_F, \quad (8)$$

$$P_s = H_D S_D D_s\left(\frac{A_k}{\Delta x}\right), \quad (9)$$

where D_s is a solute diffusivity and the A_k is a membrane porosity. Note that H_F, H_D, S_F, and S_D are the convection and diffusion steric parameters that are related to the wall correction factors of the solute (H_F and H_D), the convection and diffusion averaged distribution coefficients for steric effects only (S_F and S_D) [50]. They are given by:

$$H_F = 1 + \frac{16}{9}\eta^2, \quad (10)$$

$$H_D = 1, \quad (11)$$

$$S_F = (1-\eta)^2\left[2-(1-\eta)^2\right], \quad (12)$$

$$S_F = (1-\eta)^2, \quad (13)$$

where,

$$\eta = \frac{r_s}{r_p}. \tag{14}$$

1.1.3 Teorell-Meyer-Sievers (TMS) model

In this model, the ion concentration and electric potential have a uniform distribution in the radial direction in the membranes. At the interface between the membrane and the external solution, the Donnan equilibrium was assumed [51]. Analysis of experimental uncharged solute rejection alone cannot provide useful quantitative data about the NF membranes with negatively surface charge. It is because the transport mechanism in NF membranes is mainly due to the combination of sieving and Donnan exclusion. Therefore, to quantitatively analyze electrical properties TMS model was employed. TMS model is a rigorous approach that has been widely used to describe the membrane electrical properties by assuming a uniform radial distribution of fixed charges and mobile species [52]. By combining the extended Nernst-Planck equation and the Donnan equilibrium theory, membrane parameters σsalt and Psalt can be determined for a mono-mono type electrolyte in aqueous feed solution as follows:

$$\sigma_s = 1 - \frac{2}{(2\alpha - 1)\zeta + \left(\zeta^2 + 4\right)^{0.5}}, \tag{15}$$

$$P_s = D_s\left(1 - \sigma_s\right)\left(\frac{A_k}{\Delta x}\right), \tag{16}$$

where,

$$\zeta = \frac{\phi X}{C_m}. \tag{17}$$

1.2 Characterization of nanofiltration membranes

1.2.1 Real rejection based on concentration polarization model

The rejection characteristics of a membrane are described by observed rejection, R_{obs} and real rejection, R_{real}. In the membrane separation processes, the concentration on the membrane surface is always higher than in the bulk due to concentration polarization which. A concentration on the membrane surface is not directly obtained from experiment thus Eqs. (18)–(20) were applied [53]:

$$\ln\left(\frac{1 - R_{obs}}{R_{obs}}\right) = \ln\left(\frac{1 - R_{\text{real}}}{R_{\text{real}}}\right) + \frac{J_v}{k}, \tag{18}$$

$$R_{obs} = \left[1 - \frac{C_p}{C_b}\right], \tag{19}$$

$$R_{\text{real}} = \left[1 - \frac{C_p}{C_w}\right] \times 100, \tag{20}$$

where; C_p is the salt concentration in permeate; C_b is the salt concentration in bulk and C_w is the salt concentration in wall.

Mass transfer coefficient, k has been found to be a function of the stirring speed and thus from the mass transfer correlation for a stirred cell, k can be written as a function of ω as in Eqs. (21)–(23) [54, 55]:

$$k = k'\omega, \tag{21}$$

$$k = k'\omega^{0.567}, \tag{22}$$

$$k' = 0.23\left(\frac{r^2}{\upsilon}\right)^{0.567}\left(\frac{\upsilon}{D_{i,\infty}}\right)^{0.33}\frac{D_{i,\infty}}{r}, \tag{23}$$

where r is the radius of stirred cell (0.051 m), υ is the kinematic viscosity (8.9×10^{-7} m^2/s), $D_{i,\infty}$ is the bulk diffusivity (m^2/s) and ω is the stirring speed, 1/s.

1.2.2 Structural details and key properties

Pore radius on the membranes surface

20 samples of flat-sheet NF membranes used throughout this study were cast at fixed shear rates (155.55 1/s) from our developed dope formulation. Based on the phase inversion process, the membranes were prepared according to the steps involved in the preparation of integrally-skinned asymmetric membrane by using dry/wet phase separation process [56]. In order to determine the pore radius of these membranes, the membranes parameters that are η, σ, H_F, S_F and S_D were determined. Spiegler-Kedem equation was employed to determine the value of reflection coefficient, σ which is reflects to the fraction of membranes pores that are smaller than the molecules in feed solution which allowed the estimation of membranes performances. Subsequently, the steric-hindrance parameters were calculated by using the Eq. (9) and Eq. (10). According to the SHP model, these parameters contributed significantly to the membranes transport mechanism for nanofiltration membranes. These effects were considered and represented in terms of diffusion and convection which is contributes to the ions transport through nanofiltration. Using the relation of $\eta = r_s/r_p$, the membranes pore radius can be measured [43, 46, 48].

Solute permeability and effective membranes thickness

The solute permeability was estimated based on Eq. (8) with the solute diffusivity as 1.61×10^{-9} m^2/s which was predicted by the Stokes-Einstein equation [57, 58]. Meanwhile, the membrane thickness can be deducted from the equation $P_s = D_s/\Delta x$ where the P_s is a solute permeability, D_s is a diffusion coefficient and Δx is a membrane thickness.

Porosity and ratio of effective membranes thickness to porosity

Membrane porosity was depending on the solute permeability, effective membrane thickness and solute diffusion coefficients. No surface pores could be visually observed in the skin of any developed NF membrane under SEM at magnification up to 5000. The assumption made in order to use the SHP model was that the transport of water and solute took place through pores of radius, r_p. Based on the Eqs. (7)–(11), the membranes porosity was estimated. The SHP model was rearranged to get another equation that allows the determination of the membranes parameter. This parameter is a ratio of effective membranes thickness to membrane porosity, $\Delta x/A_k$. That equation can be written as:

$$\frac{\Delta x}{A_k} = \frac{H_D S_D D_S}{P_s}. \tag{24}$$

By inserting all numerical values into Eq. (24), the membrane porosity, and the ratio of effective membrane thickness to membrane porosity of the various membranes at different PVP concentrations were obtained.

Effective charge density and ratio of fixed charge density to bulk concentration

In order to determine the effective membrane charge density X_d, the TMS model is used instead of the SHP model. This is because the SHP model only considered the steric-hindrance effects. The membrane charge density is an electrical property of the membrane according to the permeation experimental data. Based on the TMS model, it is worth mentioning that only the electrostatic effect is considered for the permeation of electrolytes, such as sodium chloride. In this study, the NF membranes produced were assumed as model charged porous membranes. The electrostatic effects are represented by the ξ, that is a ratio of the fixed charge density (X_d) to the bulk concentration of electrolyte (C_{total}). Using Eq. (14) and Eq. (15) and by the numerical method, the electrical effects can be determined.

2 Materials and method

2.1 Materials

Polyethersulfone (Radel A300) purchased from Amoco Chemicals, was used as a membrane material. N-methyl-2-pyrrolidone (NMP, > 99 %) and poly(vinyl pyrrolidone) (PVP K15) were purchased from Merck, Darmstadt, Germany were used as solvent and additives, respectively, while distilled water was used as a non-solvent. Water used as a coagulation medium. Sodium chloride (NaCl) and multivalence salts that are Na_2SO_4, $MgSO_4$ and $MgCl_2$ were used for nanofiltration performances test. Uncharged neutral solutes that are glycerol, glucose, saccharose, raffinose and PEG 1000 from Aldrich were used to characterize the membranes structural parameters and properties.

2.2 Formulation of polymer solutions

Equilibrium thermodynamic data on ternary system (polymer/solvent/non-solvent) was determined by a turbidimetric titration method. 100g of polymer solution (polymer/solvent) was titrated with non-solvent until the cloud point is observed. At the cloud point, the polymer solution changes from clear to turbid condition. Therefore, equilibrium composition of dope solution consisting of polymer, solvents and non-solvent can be determined. Titration was conducted at temperature of 30 °C ± 2 and 84 % humidity, until permanent turbidity was detected visually.

2.3 Dope preparation and membrane fabrication

In this study, the casting solution was prepared by the polymer concentration of 20.42 wt%. Firstly, PES was dried for at least 24 hours in a vacuum oven at a temperature of about 100±1 °C in order to remove all absorbed water vapor. PES was dissolved at about 56 °C in a multi-component solvent. The polymer solution was put into an ultrasonic bath for about 3 hours to remove the bubbles and then was kept at room temperature for 24 hours. Based on the dry/wet phase inversion technique, membranes were cast using of high precision membranes casting machine. The membranes were cast on a glass plate at ambient temperature and membranes casting condition was fixed at about 10 s of casting time, 150 μm of casting thickness. NF membranes were cast at shear rates of 155.55 1/s. Subsequently, the membranes were immersed into an aqueous bath and remained there for 1 day. For solvent-exchange process, membranes were immersed into methanol for a day and after drying process, they are ready to be used.

2.4 Experimental analysis

Nanofiltration permeation test was carried out using filtration cell (Model Milipore) with membrane effective area of about 1.39×10^{-3} m^2. Prior to the each nanofiltration test, membrane was subjected to be pressurized till about 500 kPa for 1 hour. The flux was equilibrated for the passage of the first 20 ml permeate whilst the following 20 ml permeate was collected for concentration analysis. All the results presented are averaged data obtained through five membranes samples with a variation of about ±10 %. The permeate was collected and weight is measured by an electronic balance for every minute.

2.4.1 Pure Water Permeation (PWP), volume flx (J_v) and observed rejection (R_{obs})

Using of a filtration cell (Model Milipore), circular disk membranes were cut and mounted in a stainless steel, cylindrical membrane test cell by a porous support and tightened by a rubber O-ring. Effective area of the membrane mounted under the cell is 1.39×10^{-3} m^2. At seven different operating pressures that are 300 kPa, 350 kPa, 400 kPa, 450 kPa and 500 kPa, the PWP and volume flux were for the fabricated membranes were measured. The flux and observed rejection were determined for each operating condition.

In order to reduce the polarization effects, the stirring speed was fixed at 400 rpm or 41.881 rad/sec. After each permeation test, NF membranes surface was rinsed with distilled water. The pure water permeability was measured to ensure the original flux (pure water) was recovered before next permeation test. The feed concentration of each salt solution was also fixed at 0.01M. For the flux and rejection calculation purposes, the salt concentration for all sample in feed and permeate steam were measured using a conductivity meter (Model Hach SENSION5).

2.4.2 Multivalence salts (Na_2SO_4, $MgSO_4$ and $MgCl_2$)

The permeation test for multivalences salts were conducted similar to the procedure as in previous section. Conducted at the operating pressure from 300 kPa to 500 kPa, the multivalences salt permeation test also carried out by using 0.01 M salts concentration. The feed, permeate and retentate concentration for each sample also measured by using conductivity meter. The rejection characteristics of a membrane are described in terms of observed rejection, Robs and real rejection, R_{real}.

2.4.3 Solutes separation test and morphology

The solutes concentrations of neutral solutes were (glycerol, sucrose, saccharose, raffinose and PEG 1000) were measured with a Total Organic Carbon (TOC) analyzer from Thermo Scientific.

3 Result and discussion

3.1 Effect of PVP on performances & separation characteristics

In this study, the best formulation of ternary components consisting of (PES/NMP/H_2O)-(20.42/70.06/9.52) wt/wt% was used as dope solution. Using of this formulation, the addition of the polymeric additives in dope solutions was studied. For this purpose, the enhanced polymeric additive that is poly(vinyl pyrrolidone) (PVP K15) in the ranges of 2.0 to 10.0 wt% was used as a porosity enhancer. Then, the effect of PVP concentration in dope solution on performances, structural details and key properties NF membranes were examined based on the modeling method. The membranes types and casting conditions induced in this study was tabulated in Table 1.

Using of our best developed dope formulation, the NF membranes were cast by using of our high precision membranes casting system at different shear rates. The membranes had been evaluated in terms of PWP, NaCl permeation and rejection efficacy. Multivalence salts that are Na_2SO_4, $MgSO_4$ and $MgCl_2$ are used to verify the membranes separation performances. Fig. 1 shows the PWP results of the NF membranes at different concentration of PVP. From the graph, it was clear that the highest PWP achieved of about 14.15×10^{-6} m^3/m^{2}s performed by the PVP 6 wt% membranes while the PVP 10 wt% membranes showed the lowest PWP of about 8.94×10^{-6} m^3/m^{2}s. In general, the increasing of PVP concentration from 2–6 wt% in dope solution causes to a higher water permeability while the larger amount of PVP from 8–10 % produced lower water permeation membranes.

Table 1 Casting condition of NF membranes at different PVP concentration

Membranes type	Casting time (s)	Shear rates γ (1/s)	PVP (wt%)
NF202	15	155.55	2
NF204	15	155.55	4
NF206	15	155.55	6
NF208	15	155.55	8
NF2010	15	155.55	10

* Membrane length = 35.00 cm and thickness 150 μm (0.015 cm)

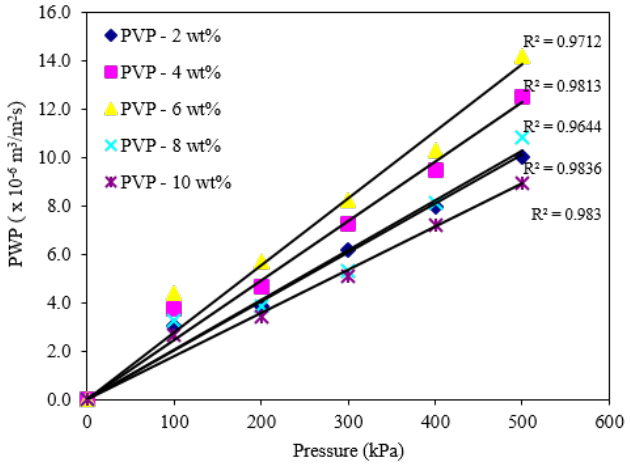

Fig. 1 Pure Water Permeation (PWP) of NF membranes at different operating pressure

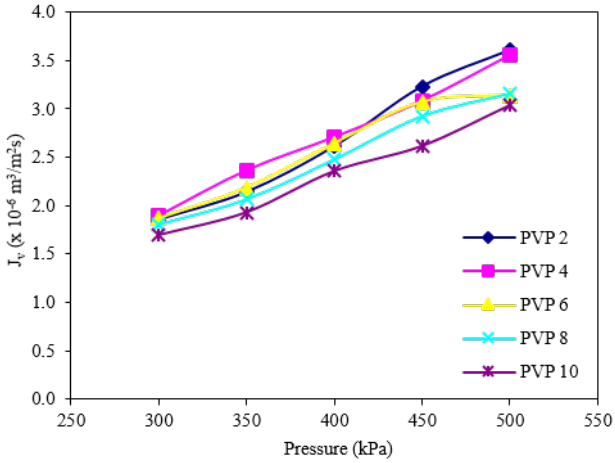

Fig. 2 Volume flux, J_v of NF membranes at different PVP concentrations

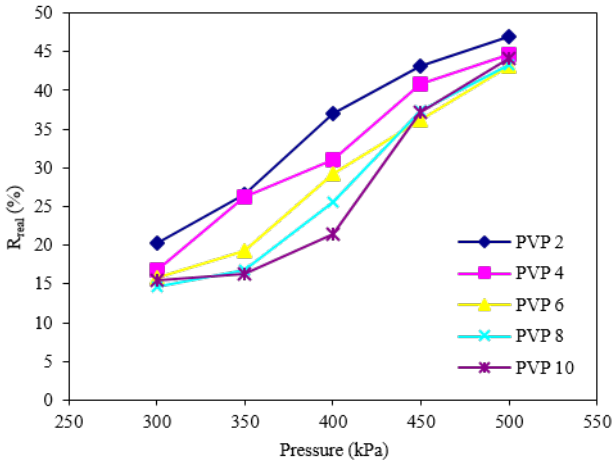

Fig. 3 Real rejection, R_{real} of NF membranes at different PVP concentrations

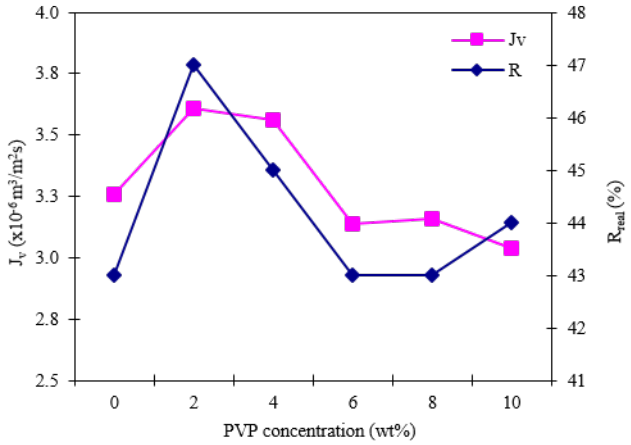

Fig. 4 J_v and R_{real} of 0.01M NaCl at different PVP concentrations and 500 kPa of operating pressure

Using of the established Milipore permeation cell, the membranes performances was evaluated in terms of PWP, fluxes and salts rejection and neutral solutes separation were tested under operating pressure of 500 kPa. The permeation experiment was performed by using 0.01M NaCl and 300 ppm of neutral solutes. Multivalences salt that are Na_2SO_4, $MgSO_4$, and $MgCl_2$ had been used for performance verifications. For the modeling purposes, the ionic data of different salts are summarized in Table 2.

Figs. 2 and 3 showed the performances of fabricated NF membranes in terms of volume flux and salt rejection. In general, it was clearly observed that as pressure increased, the volume flux and salt rejection were increased. At 500 kPa of operating pressure, 2 wt% of PVP membranes showed the highest volume flux and salt rejection of about 3.61×10^{-6} m³/m²s and 44.48 %, respectively. Meanwhile, the 10 wt% of PVP membranes results the lowest volume flux of 3.04×10^{-6} m³/m²s and lowest of salt rejection of 41.12 % was demonstrated by 6 wt% PVP membranes.

In order to verify the influence of PVP concentration on the membranes performances, the data of volume flux and real rejection were plotted against additive concentration and the graph was presented as in Fig. 4. This graph clearly showed the performances trends of the fabricated NF membranes. The highest salt rejection and volume flux was demonstrated by 2 wt% PVP membranes. With the salt rejection of about 44.48 % and volume flux of about 3.61×10^{-6} m³/m²s, the 2 wt% PVP (NF202) was found to be the optimum PVP concentration. Beyond the 2 wt% of PVP concentration, membranes volume flux and salt

Table 2 Diffusion coefficient and solute size for ions

Ions	$D_\infty \times 10^{-9}$ (m²/s)	r_s (nm)
Na+	1.33	0.18
Mg^{2+}	0.70	0.35
Cl-	2.01	0.12
SO_4^{2-}	1.06	0.23

rejection reduced significantly to the lowest volume flux by 10 wt% PVP membranes. This separation profiles may be due to the suppression of macrovoids, well interconnected membranes structures and the formation of thicker membrane skin layer [33, 59].

The researchers reported that the addition of polymer additive PEG which is sufficient to drive the composition of dope solution to be closed to the precipitation point (cloud point). With increasing of polymer additive concentration, the coagulant tolerance is lowered due to the highly entangled solution conformation thus resulted in a decreased of flux [60]. By adding the additive, the polymer solution became unstable and the solvents located between the polymers chains can be easily diffused out to the coagulation bath. Therefore, polymeric additives can suppress the formation of macrovoids beneath skin layer and pores became very well interconnected [61]. Besides, the effect of PVP additive on the membranes also reported by the previous researchers [17, 33].

Fig. 5 showed the rejection of multivalences salts against additive concentration. Different types of salts that are Na_2SO_4, $MgSO_4$, and $MgCl_2$ were used for the performances evaluation as comparison to the NaCl removal. Generally, the fabricated NF membranes showed a very good rejection of multivalent salts. It is clearly observed that, the PVP 2 wt% membranes demonstrated for almost up to 91 % of multivalent salts. The highest rejection achieved of about 91.02 % for $MgSO_4$, revealed that the used of small amount of PVP additives in dope solution tended to produce more selective membranes. Moreover, the PVP concentrations from 8–10 wt% in dope solution are found to be not effective due to the inverse permeation trends and separation profiles. Real rejection sequences for

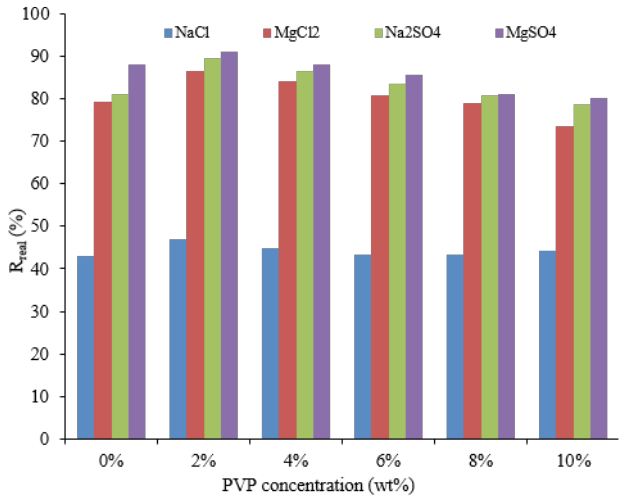

Fig. 5 Graf R_{real} of multivalent salts for the optimum membranes

all membranes were $MgSO_4$ > Na_2SO_4 > $MgCl_2$ > NaCl. This rejection trend is similar to the previous data at different polymer concentration NF membranes.

The sequence of the salts rejection could be explained by considering of ions properties that diffusion coefficient (D_∞) and solute size (r_s). As shown in Table 2, the ion diffusivity (D_∞) follows the sequences of Cl- > K+ > Na+ > SO_4^{2-} > Mg^{2+} while the solute size follows the order of Mg^{2+} > SO_4^{2-} > Na+ > K+ > Cl-. The trends could explain why the real rejection profiles shown in Fig. 5 were obtained. Higher diffusivity and smaller solute size could enhance mass transport through the membrane materials. Higher solute transport resulted in poorer rejection of the membranes. According to the Donnan exclusion theory, a higher valence counter-ion leads to a lower rejection of the salt [62]. Such results also were reported by other researchers [63, 64]. Therefore, it can be proposed that 2 wt% of PVP is the optimum PVP concentration for the highly permeable NF membranes.

3.2 Effect of PVP on membranes parameter & structural properties

Prior to further analyze on the key properties and structural details, the membranes parameters that are reflection coefficients, σ, solute permeability, P_s, ratio of solute radius to pore radius, r_s/r_p, ratio of membranes thickness to porosity, $\Delta x/A_k$ and pore radius, rp of the fabricated NF membranes were determined based on the Spiegler-Kedem equation and Steric-Hindrance Pore (SHP) model. Table 3 summarized the overall results of structural parameters and properties for the fabricated NF membranes at different PVP concentrations.

In general, modeling results showed that the increasing of solutes molecular weight caused to the decreasing of solutes permeability and changes of membranes pore radius. However, the overall data showed that the structural parameters and properties of the fabricated NF membranes are in the ranges of nanofiltration membranes. It was found that the at the optimum PVP concentration of about 2 wt% a good membranes parameters and structural properties of r_p and $\Delta x/A_k$ ranges from 1.03 nm to 1.53 nm and 9.05 μm to 103.44 μm are the main factors contributed to the highest permeation and salt rejection.

In addition, modeling data also revealed that, the increasing of PVP concentration in dope solution produced larger pore radius which is significantly resulted to the higher solutes permeability. Meanwhile, the higher PVP concentration also found to cause to the higher figure of reflection

Table 3 Structural parameters and properties of NF membranes at different PVP concentrations (wt%)

Membranes NF	Neutral solutes	Membrane parameters & properties					
		σ (-)	P_s (10^{-7} m/s)	r_p (nm)	η (rs/rp)	$A_k/\Delta x$ (1/m)	$\Delta x/A_k$ (μm)
NF202	Glycerol	0.29	3.94	1.53	0.17	732	103.44
	Glucose	0.36	2.35	1.66	0.22	676	91.37
	Saccharose	0.50	1.75	1.41	0.33	913	66.67
	Raffinose	0.60	1.24	1.36	0.43	1080	48.98
	PEG 1000	0.86	0.38	1.03	0.75	2960	9.05
NF204	Glycerol	0.15	5.67	3.21	0.08	861	126.67
	Glucose	0.21	4.50	3.11	0.12	1010	116.87
	Saccharose	0.34	3.15	2.30	0.21	1160	94.85
	Raffinose	0.43	2.22	2.13	0.27	1200	79.09
	PEG 1000	0.63	1.66	1.70	0.46	2710	43.76
NF206	Glycerol	0.13	6.75	3.74	0.07	999	129.87
	Glucose	0.19	5.01	3.48	0.10	1100	120.16
	Saccharose	0.31	4.04	2.58	0.18	1410	100.02
	Raffinose	0.37	2.83	2.57	0.23	1350	89.63
	PEG 1000	0.53	2.12	2.17	0.36	2470	61.34
NF208	Glycerol	0.10	7.94	4.94	0.05	1130	134.63
	Glucose	0.13	6.52	5.25	0.07	1320	129.87
	Saccharose	0.25	5.01	3.30	0.14	1590	110.20
	Raffinose	0.31	3.42	3.18	0.18	1470	100.02
	PEG 1000	0.45	2.59	2.70	0.29	2450	75.55
NF2010	Glycerol	0.07	10.30	7.17	0.04	1420	139.32
	Glucose	0.09	7.82	7.75	0.05	1510	136.20
	Saccharose	0.22	6.19	3.81	0.12	1870	115.21
	Raffinose	0.26	3.92	3.91	0.15	1550	108.52
	PEG 1000	0.37	3.23	3.45	0.23	2570	89.63

coefficients. This parameter may also be one of the factors for the higher salt rejection for the NF membranes. The information on these technical properties is very important and according to SHP model, these parameters contributed significantly to the transport mechanism of nanofiltration process and separation performances [46, 65].

Table 4 presents the results of membranes parameters and steric hindrance factors for the fabricated NF membranes at different PVP concentrations. Based on the modeling data, the steric effects that are S_F and S_D for the ions transport through the membranes are found to be increased with the higher concentration of PVP. The 2 wt% PVP membranes show minimum values for these factors and remaining the higher hindrance factors *HF*. In the combinations with steric-hindrance factors, the 2 wt% PVP membranes also showed the highest reflection coefficients which are the main factors for the membranes to result the best separation performances. In order to support the results, the relationship between rejection and reflection coefficient values, these both values were calculated and given as in Table 5.

Table 4 Membranes parameters and steric-hindrance factors at different PVP concentrations (wt%)

Membrane parameters	PVP concentration (wt%)				
	2	4	6	8	10
η	0.31	0.29	0.27	0.27	0.28
σ	0.15	0.13	0.12	0.12	0.13
H_F	1.17	1.15	1.13	1.13	1.14
S_F	0.73	0.75	0.78	0.78	0.77
S_D	0.48	0.50	0.53	0.53	0.52

Table 5 Values of salts rejection and reflection coefficient at different PVP concentrations (wt%)

Membrane parameters	PVP concentration (wt%)				
	2	4	6	8	10
R_{real} (%)	46.94	44.71	43.22	43.26	44.09
σ (-)	0.15	0.13	0.12	0.12	0.13

It was found that, highest reflection coefficient and salt rejection values at the 2 wt% of PVP concentration were found to be about 0.15 and 46.94 %, respectively.

As the membrane parameters and steric-hindrances factors found, the analysis on the overall properties and characteristics is needed to confirm and verify the optimum PVP concentrations. For this purpose, the set of NF membranes structural and electrical properties were summarized in Table 6. Modeling results on the electrostatics properties that are surface charged density, X_d and zeta potential, ζ values showed the highest values of about 0.03 and −1.71, respectively. As one of the important separation and transport mechanism in nanofiltration membranes, the values of both parameters are important and cannot be neglected.

Considering of the overall performances and properties of the fabricated NF membranes, the optimum PVP concentration was found to be at about 2 wt% and the best membranes is NF202. Hereby, it can be concluded that the use of enhanced polymeric additives is very significant to improve the performances and properties of integrally NF membranes. As an optimum polymer concentration, the optimum additives concentration could be defined as a maximum value in which the resultant membrane exhibited optimal performances (in terms of salt rejection and permeation flux), good morphologies and also provided the best separation properties. At this point, membranes properties such as rejection, flux, pore radius and membrane charge exhibited good values. Beyond the optimum concentration, the membranes properties, separation characteristics and structural details are vice versa.

Miscibility with membrane materials and soluble in water as well as solvents makes PVP one of a good polymer additive [8]. In fact, it has been widely studied that PVP is added to polymer solutions as a micropores promoter during membranes formation. During the phase inversion process, it is assumed that the hydrophilic additive, PVP is dissolved out by water and sites where the PVP exist became micro pores. As the membranes structural details and membranes properties were characterized and quantitatively measured, there is the need to identify the relationships amongst them. For this purpose, the selected performances and membranes properties data that are, volume flux, real rejection, pore radius, ratio of thickness to porosity, charge density and zeta potential values are correlate. This idea promotes to the new finding of technical specifications for the membranes production and application.

Table 6 Membranes structural properties at different PVP concentrations (wt %)

Membrane properties	PVP concentration (wt %)				
	2	4	6	8	10
Ps × 10^{-7} (m/s)	2.68	2.69	2.41	2.42	2.31
A_k	2.08	1.99	1.90	1.90	1.94
r_p (nm)	1.41	2.49	2.91	3.87	5.22
$\Delta x/A_k$ (μm)	9.05	4.38	61.30	75.51	89.63
X_d	0.030	0.027	0.026	0.026	0.027
ζ (-)	1.71	1.63	1.56	1.57	1.60

Figs. 6–9 showed the relations of volume flux, J_v and membranes key properties at different PVP concentrations. From the graph it was shown that the volume flux, J_v of NF membranes is strongly influenced by pore radius, r_p and $\Delta x/A_k$. Low concentrations of PVP (below than 4 wt%) in dope solutions produced a smaller pore radius and $\Delta x/A_k$ values. This is a main reason where the highest J_v was performed by the 2 wt% PVP membranes. This finding corresponds to the previous studies which reported that at the optimum PVP concentration membranes skin layer thickness was tend to be reduced.

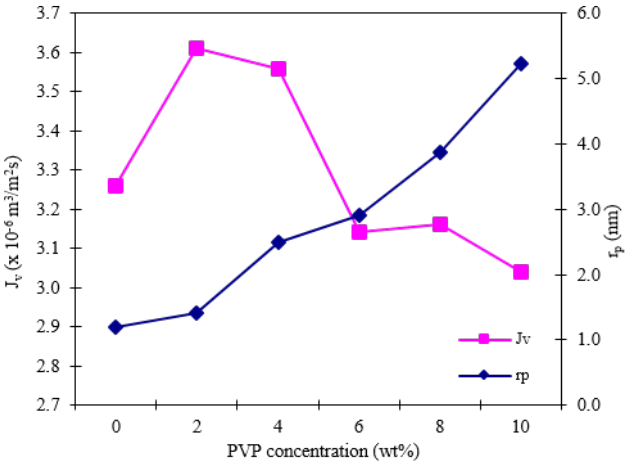

Fig. 6 Effects of pore radius, r_p on volume flux, J_v at different PVP concentrations

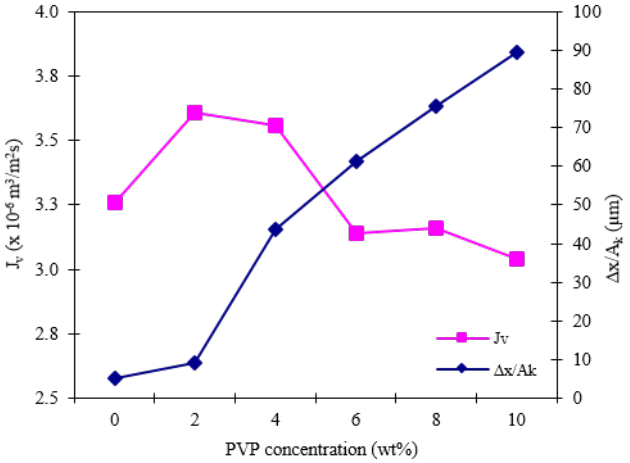

Fig. 7 Effects of $\Delta x/A_k$ on volume flux, J_v at different PVP concentrations

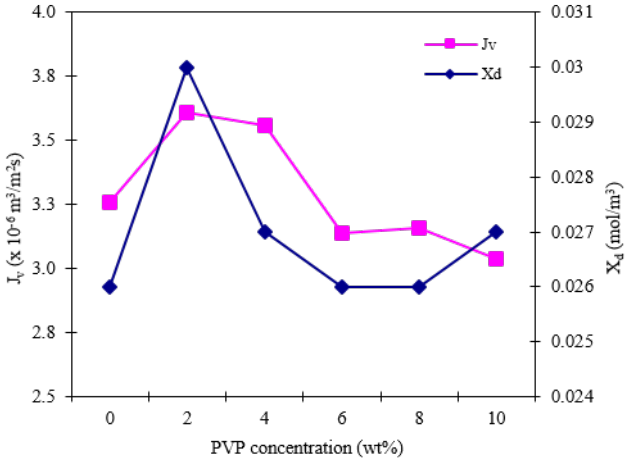

Fig. 8 Effects of surface charge density, X_d on volume flux, J_v at different PVP concentrations

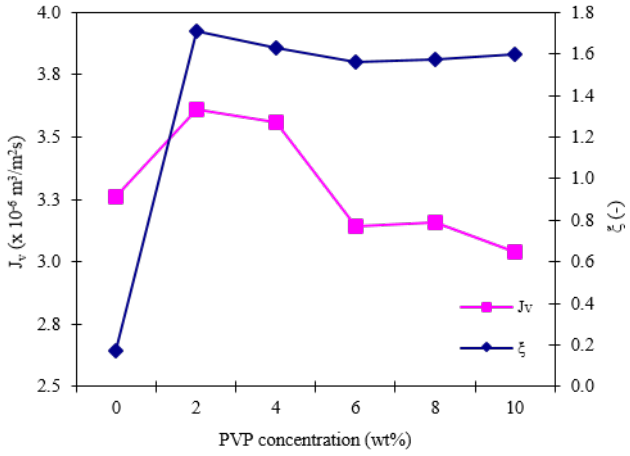

Fig. 9 Effects of zeta potential, ζ on volume flux, J_v at different PVP concentrations

Decreasing of skin layer thickness will reduce the membrane resistance and provide a selective active layer for the permeation and separation process. In fact, thinner skin layer possesses better membranes performances and the reduction of skin layer thickness caused an increasing of salt rejection [52]. Furthermore, at the optimum PVP concentration of 2 wt%, NF membranes demonstrated the highest values charge density, X_d and zeta potential, ζ. Thus, it was verified that the membranes properties are influenced and highly reflected to the membranes permeability [42].

Meanwhile, analysis on the rejection characteristics from Figs. 10–12 revealed that the membranes key properties found to be strong factors to the separation performances features. As 2 wt% PVP membranes demonstrated the highest volume flux, the same factor that smallest pore radius was found to drive the membranes to achieve highest separation performances. The increasing of pore radius with the higher PVP concentration led to the reduction of

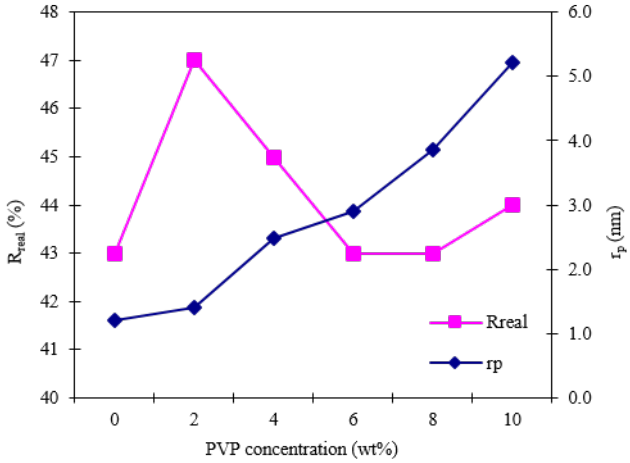

Fig. 10 Effects of pore radius, r_p on real rejection, R_{real} at different PVP concentrations

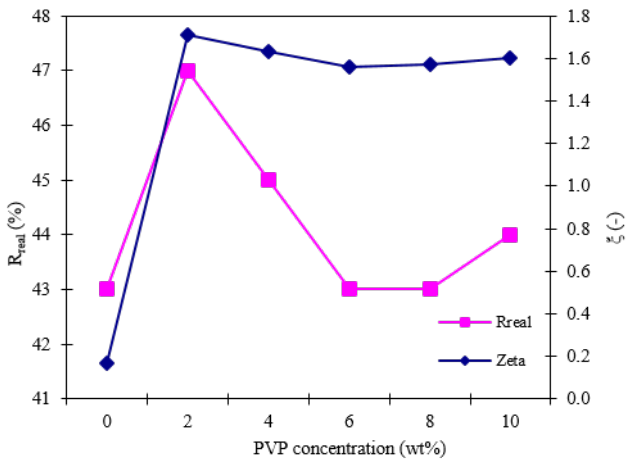

Fig. 11 Effects of zeta potential, ζ on real rejection, R_{real} at different PVP concentrations

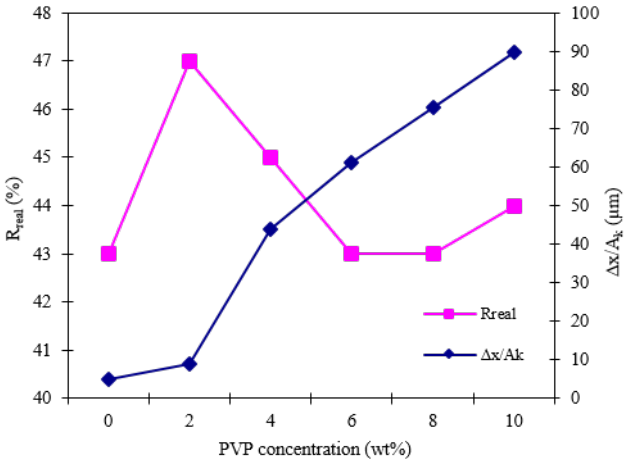

Fig. 12 Effects of $\Delta x/A_k$ on real rejection, R_{real} at different PVP concentrations

salt rejection. It is found that the highest surface charge, ζ at the 2 wt% PVP also promoted to the highest performances of ALP-NF202 membrane.

As pore radius size was found to be one of the utmost important parameters influences to the membrane performances, the significant relation between pore radius and porosity parameter that is $\Delta x/A_k$ was investigated. For this intention, the modeling data for both parameters was plotted as ion Fig. 13. It was clearly observed that, the ratio of thickness to porosity $\Delta x/A_k$ and pore radius, r_p parameters were found to be increased proportionally with the increasing of PVP concentration. Therefore, this finding also provided a significant support to the 2 wt% of PVP to be the optimum concentration for the fabrication of high selective NF membrane.

As a comparison to the membrane properties, the modeling results obtained was compared to the available commercial nanofiltration membranes. Key properties of the 29 commercial NF membranes in terms of pore radius, surface charge and ratio of thickness to porosity were summarized as in Table 7. It is pleased to say that the properties of the fabricated NF202 membranes are found to be in the ranges of commercial NF membranes.

4 Conclusions

The assessment on the performances, structural details and key properties of the fabricated NF membranes provided a good input of membranes technical properties and better understanding on the effect of poly(vinyl pyrrolidone) (PVP) for the fabrication of NF membranes. Based on this study, the following conclusions have been made:

1. The addition of PVP additive into dope solution significantly altered the properties and membranes structures thus directly affected the separation performances of NF membranes.
2. The small amount of PVP additive (2 wt%) produced the optimum NF membranes with highest rejection capability and finest properties.
3. The presence of PVP additive into dope and for fabrication of asymmetric membranes was also found affected the electrical properties that are effective charge density, X_d and membrane surface charge, ζ (zeta potential).
4. The used of poly(vinyl pyrrolidone), PVP as additive was found to be very useful towards the separation improvement and properties enhancement.

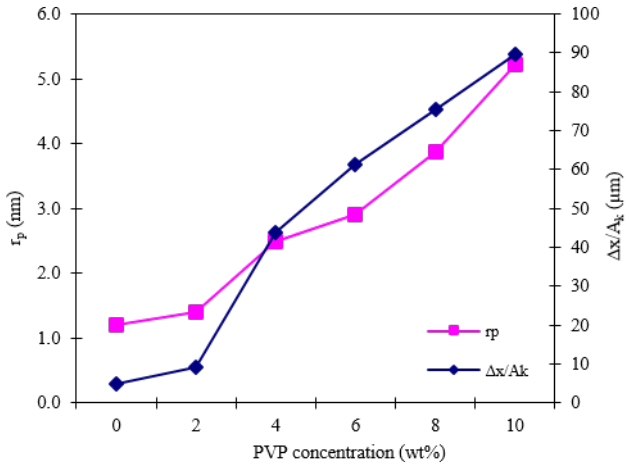

Fig. 13 Effects of PVP concentrations on r_p and $\Delta x/A_k$ at different PVP concentrations

Table 7 Summary of the 29 commercial NF and fabricated NF membrane at optimum PVP concentration (wt %)

Properties	r_p (nm)	ζ (-)	$\Delta x/A_k$ (μm)
Minimum	0.39	1.5	0.66
Mean	0.66	9.2	4.8
Maximum	1.59	44.5	16.9
NF202	1.41*	1.71*	9.05*

* Mean values of modeling results

Acknowledgment

The authors wish to express their gratitude to the Center for Research Excellence and Incubation Management (RMIC), Universiti Sultan Zainal Abidin (UniSZA) and East Institute of Oceanography and Environment (INOS), Universiti Malaysia Terengganu (UMT) for their assistance on instrumental analysis.

Nomenclature

A_k membrane porosity
c concentration (mol/m^3)
c_i concentration of component i (mol/m^3)
c_m electrolyte concentration at the membrane surface
$c_{p,i}$ concentration of component i in the permeate (mol/l)
$c_{r,i}$ concentration of component i in the rejection (mol/l)
C_{total} total charge concentration in bulk solution (of –ve or +ve solutes) (mol/m^3)
D_i diffusivity of ion i in free solution (m^2/s)
D_s solute diffusivity for neutral molecule, or generalized diffusivity for 1-1 type of electrolyte defined as $D_s = 2(D_1D_2)/(D_1 + D_2)$ (m^2/s)
F Faraday constant (= 96487) (C/mol)
H_F, H_D steric parameters related to wall correction factors under diffusion and convection conditions, respectively (-)
J_s averaged solute flux over membrane surface (mol/m^{2}s)
J_v averaged volume flux over membrane surface (m/s)
k_i averaged distribution coefficients of ion i by the electrostatic effects

P_s solute permeability (m/s)
r pore size (m)
r_p pore radius (m)
r_s solute radius (m)
R_i rejection of component i (%)
R rejection, or gas constant (8.314)(J/mol^3 K)
S_F, S_D distribution coefficients of solute by steric-hindrance effect under diffusion and convection condition, respectively (-)
X_d effective membrane charge density (mol/m^3)
z_i valence of ion
ΔP applied pressure (Pa)
Δx membrane thickness (m)
$\Delta x/A_k$ ratio of membrane thickness to membrane porosity
ϕX effective volume charge density

Greek

ε membrane porosity (dimensionless)
ξ ratio of fixed charge density to salt concentration
σ reflection coefficient (%)
η viscocity of solution (Pa s)
τ tortuosity (dimensionless)

References

[1] Qasim, M., Badrelzaman, M., Darwish, N. N., Darwish, N. A., Hilal, N. "Reverse osmosis desalination: A state-of-the-art review", Desalination, 459, pp. 59–104, 2019. https://doi.org/10.1016/j.desal.2019.02.008

[2] Bagheripour, E., Moghadassi, A. R., Parvizian, F., Hosseini, S. M., Van der Bruggen, B. "Tailoring the separation performance and fouling reduction of PES based nanofiltration membrane by using a PVA/Fe3O4 coating layer", Chemical Engineering Research and Design, 144, pp. 418–428, 2019. https://doi.org/10.1016/j.cherd.2019.02.028

[3] Galiano, F., Briceño, K., Marino, T., Molino, A., Christensen, K. V., Figoli, A. "Advances in biopolymer-based membrane preparation and applications", Journal of Membrane Science, 564, pp. 562–586, 2018. https://doi.org/10.1016/j.memsci.2018.07.059

[4] Jalali, A., Shockravi, A., Vatanpour, V., Hajibeygi, M. "Preparation and characterization of novel microporous ultrafiltration PES membranes using synthesized hydrophilic polysulfide-amide copolymer as an additive in the casting solution", Microporous and Mesoporous Materials, 228, pp. 1–13, 2016. https://doi.org/10.1016/j.micromeso.2016.03.024

[5] Nikooe, N., Saljoughi, E. "Preparation and characterization of novel PVDF nanofiltration membranes with hydrophilic property for filtration of dye aqueous solution", Applied Surface Science, 413, pp. 41–49, 2017. https://doi.org/10.1016/j.apsusc.2017.04.029

[6] Zainal, S. H., Hassan, A. R., Isa, M. H. M. "The Effect of Polymer Concentration and Surfactant Types on Nanofiltration-Surfactant Membrane for Textile Wastewater", Malaysian Journal of Analytical Sciences, 20(6), pp. 1524–1529, 2016. https://doi.org/10.17576/mjas-2016-2006-34

[7] Ladewig, B., Al-Shaeli, M. N. Z. "Fundamentals of Membrane Processes", In: Fundamentals of Membrane Bioreactors, Springer, Singapore, 2017, pp. 13–37. https://doi.org/10.1007/978-981-10-2014-8_2

[8] Singh, R. "Introduction to membrane technology", In: Singh, R. (ed.) Membrane Technology and Engineering for Water Purification, Membrane Ventures, LLC, Colorado Springs, CO, USA, 2015, pp. 1–80. https://doi.org/10.1016/B978-0-444-63362-0.00001-X

[9] Purkait, M. K., Sinha, M. K., Mondal, P., Singh, R. "Introduction to membranes", In: Pukrait, M. K., Sinha, M. K., Mondal, P., Singh, R. (eds.) Stimuli Responsive Polymeric Membranes, Interface Science and Technology 25, Academic Press, London, UK, 2018, pp. 1–37. https://doi.org/10.1016/B978-0-12-813961-5.00001-2

[10] Sapalidis, A. A. "Porous Polyvinyl Alcohol Membranes: Preparation Methods and Applications", Symmetry, 12(6), Article number: 960, 2020. https://doi.org/10.3390/sym12060960

[11] Wang, S., Li, X., Wu, H., Tian, Z., Xin, Q., He, G., Peng, D., Chen, S., Yin, Y., Jiang, Z., Guiver, M. D. "Advances in high permeability polymer-based membrane materials for CO2 separations", Energy and Environmental Science, 9(6), pp. 1863–1890, 2016. https://doi.org/10.1039/C6EE00811A

[12] Salahi, A., Mohammadi, T., Behbahani, R. M., Hemmati, M. "Experimental investigation and modeling of industrial oily wastewater treatment using modified polyethersulfone ultrafiltration hollow fiber membranes", Korean Journal of Chemical Engineering, 32(6), pp. 1101–1118, 2015. https://doi.org/10.1007/s11814-014-0310-1

[13] Anvari, A., Safekordi, A., Hemmati, M., Rekabdar, F., Tavakolmoghadam, M., Azimi Yancheshme, A. A., Gheshlaghi, A. "Enhanced separation performance of PVDF/PAN blend membrane based on PVP tuning", Desalination and Water Treatment, 57(26), pp. 12090–12098, 2016. https://doi.org/10.1080/19443994.2015.1051123

[14] Urkiaga, A., Iturbe, D., Etxebarria, J. "Effect of different additives on the fabrication of hydrophilic polysulfone ultrafiltration membranes", Desalination and Water Treatment, 56(13), pp. 3415–3426, 2015. https://doi.org/10.1080/19443994.2014.1000976

[15] Fadilah, N. I. M., Hassan, A. R. "Preparation, Characterization and Performance Studies of Active PVDF Ultrafiltration-Surfactants Membranes Containing PVP as Additive", Advanced Materials Research, 1134, pp. 44–49, 2015. https://doi.org/10.4028/www.scientific.net/AMR.1134.44

[16] Chen, X., Tang, B., Luo, J., Wan, Y. "Towards high-performance polysulfone membrane: The role of PSF-b-PEG copolymer additive", Microporous and Mesoporous Materials, 241, pp. 355–365, 2017.
https://doi.org/10.1016/j.micromeso.2016.12.032

[17] Gebru, K. A., Das, C. "Effects of solubility parameter differences among PEG, PVP and CA on the preparation of ultrafiltration membranes: Impacts of solvents and additives on morphology, permeability and fouling performances", Chinese Journal of Chemical Engineering, 25(7), pp. 911–923, 2017.
https://doi.org/10.1016/j.cjche.2016.11.017

[18] Hassan, A. R., Takwa, C. W. I. C. W., Safari, N. H. M., Rozali, S., Sulaiman, N. A. "Characterization on Performance, Morphologies and Molecular Properties of Dual-Surfactants Based Polyvinylidene Fluoride Ultrafiltration Membranes", Periodica Polytechnica Chemical Engineering, 64(3), pp. 320–327, 2020.
https://doi.org/10.3311/ppch.13862

[19] Lee, J., Park, B., Kim, J., Park, S. B. "Effect of PVP, lithium chloride, and glycerol additives on PVDF dual-layer hollow fiber membranes fabricated using simultaneous spinning of TIPS and NIPS", Macromolecular Research, 23(3), pp. 291–299, 2015.
https://doi.org/10.1007/s13233-015-3037-x

[20] Li, X., Li, Q., Fang, W., Wang, R., Krantz, W. B. "Effects of the support on the characteristics and permselectivity of thin film composite membranes", Journal of Membrane Science, 580, pp. 12–23, 2019.
https://doi.org/10.1016/j.memsci.2019.03.003

[21] Zheng, L., Wu, Z., Wei, Y., Zhang, Y., Yuan, Y., Wang, J. "Preparation of PVDF-CTFE hydrophobic membranes for MD application: Effect of LiCl-based mixed additives", Journal of Membrane Science, 506, pp. 71–85, 2016.
https://doi.org/10.1016/j.memsci.2016.01.044

[22] Ayyaru, S., Ahn, Y.-H. "Application of sulfonic acid group functionalized graphene oxide to improve hydrophilicity, permeability, and antifouling of PVDF nanocomposite ultrafiltration membranes", Journal of Membrane Science, 525, pp. 210–219, 2017.
https://doi.org/10.1016/j.memsci.2016.10.048

[23] Otitoju, T. A., Ahmad, A. L., Ooi, B. S. "Superhydrophilic (superwetting) surfaces: A review on fabrication and application", Journal of Industrial and Engineering Chemistry, 47, pp. 19–40, 2017.
https://doi.org/10.1016/j.jiec.2016.12.016

[24] Kong, J., Li, K. "Preparation of PVDF hollow-fiber membranes via immersion precipitation", Journal of Applied Polymer Science, 81(7), pp. 1643–1653, 2001.
https://doi.org/10.1002/app.1595

[25] Mazinani, S., Darvishmanesh, S., Ehsanzadeh, A., Van der Bruggen, B. "Phase separation analysis of Extem/solvent/non-solvent systems and relation with membrane morphology", Journal of Membrane Science, 526, pp. 301–314, 2017.
https://doi.org/10.1016/j.memsci.2016.12.031

[26] Rasool, M. A., Vankelecom, I. F. J. "Preparation of full-bio-based nanofiltration membranes", Journal of Membrane Science, 618, Article number: 118674, 2021.
https://doi.org/10.1016/j.memsci.2020.118674

[27] Eren, B., Güney, M. "The role of polyvinylpyrrolidone as a pore former on microstructure and performance of polysulfone membranes", Bilecik Şeyh Edebali Üniversitesi Fen Bilimleri Dergisi, 6, pp. 168–176, 2019.
https://doi.org/10.35193/bseufbd.589808

[28] Hołda, A. K., Vankelecom, I. F. J. "Understanding and guiding the phase inversion process for synthesis of solvent resistant nanofiltration membranes", Journal of Applied Polymer Science, 132(27), Article number: 42130, 2015.
https://doi.org/10.1002/app.42130

[29] Mohd Ali, N. S.., Hassan, A. R. "The effect of CTAB and SDS surfactant on the morphology and performance of low pressure active reverse osmosis membrane", Malaysian Journal of Analytical Sciences, 20(3), pp. 510–516, 2016.
https://doi.org/10.17576/mjas-2016-2003-07

[30] Wang, D., Li, K., Teo, W. K. "Porous PVDF asymmetric hollow fiber membranes prepared with the use of small molecular additives", Journal of Membrane Science, 178(1–2), 13–23, 2000.
https://doi.org/10.1016/S0376-7388(00)00460-9

[31] Wang, D., Li, K., Teo, W. K. "Relationship between mass ratio of nonsolvent-additive to solvent in membrane casting solution and its coagulation value", Journal of Membrane Science, 98(3), pp. 233–240, 1995.
https://doi.org/10.1016/0376-7388(94)00191-Z

[32] Sangeetha, M. S., Kandaswamy, A., Vijayalakshmi, A. "Preparation and Characterisation of Flat Sheet Micro/Nanoporous Membranes Using Polysulfone Blend with PVP/PEG and Chitosan/Chitosan Nanoparticles for Biomedical Applications", Journal of Optoelectronics and Biomedical Materials, 8(2), pp. 81–87, 2016.

[33] Kourde-Hanafi, Y., Loulergue, P., Szymczyk, A., Van der Bruggen, B., Nachtnebel, M., Rabiller-Baudry, M., Sudic, J.-L., Baddari, K. "Influence of PVP content on degradation of PES/PVP membranes: Insights from characterization of membranes with controlled composition", Journal of Membrane Science, 533, pp. 261–269, 2017.
https://doi.org/10.1016/j.memsci.2017.03.050

[34] Sulaiman, N. A., Hassan, A. R., Rozali, S., Safari, N. H. M., Takwa, C. W. I. C. W., Mansoor A, A. D. K., Md Saad, M. H. "Development of Asymmetric Low Pressure Reverse Osmosis-Surfactants Membrane: Effect of Surfactant Types and Concentration", Periodica Polytechnica Chemical Engineering, 64(3), pp. 296–303, 2020.
https://doi.org/10.3311/PPch.13327

[35] Son, M., Kim, H., Jung, J., Jo, S., Choi, H. (2017). "Influence of extreme concentrations of hydrophilic pore-former on reinforced polyethersulfone ultrafiltration membranes for reduction of humic acid fouling", Chemosphere, 179, pp. 194–201, 2017.
https://doi.org/10.1016/j.chemosphere.2017.03.101

[36] Tofighy, M. A., Mohammadi, T., Sadeghi, M. H. "High-flux PVDF/PVP nanocomposite ultrafiltration membrane incorporated with graphene oxide nanoribbones with improved antifouling properties", Journal of Applied Polymer Science, 138(4), Article number: 49718, 2021.
https://doi.org/10.1002/app.49718

[37] Lee, A., Elam, J. W., Darling, S. B. "Membrane materials for water purification: design, development, and application", Environmental Science: Water Research and Technology, 2(1), pp. 17–42, 2016. https://doi.org/10.1039/C5EW00159E

[38] Epsztein, R., Shaulsky, E., Dizge, N., Warsinger, D. M., Elimelech, M. "Role of Ionic Charge Density in Donnan Exclusion of Monovalent Anions by Nanofiltration", Environmental Science and Technology, 52(7), pp. 4108–4116, 2018. https://doi.org/10.1021/acs.est.7b06400

[39] Ji, Y.-L., Gu, B.-X., An, Q.-F., Gao, C.-J. "Recent Advances in the Fabrication of Membranes Containing "Ion Pairs" for Nanofiltration Processes", Polymers, 9(12), Article number: 715, 2017. https://doi.org/10.3390/polym9120715

[40] Nakao, S.-I., Kimura, S. "Models of membrane transport phenomena and their applications for ultrafiltration data", Journal of Chemical Engineering of Japan, 15(3), pp. 200–205, 1982. https://doi.org/10.1252/jcej.15.200

[41] Ali, N., Hassan, A. R., Wong, L. Y. "Development of novel asymmetric ultra low pressure membranes and a preliminary study for bacteria and pathogen removal applications", Desalination, 206(1–3), pp. 474–484, 2007. https://doi.org/10.1016/j.desal.2006.02.074

[42] Yunos, K. F. M., Mazlan, N. A., Naim, M. N. M., Baharuddin, A. S., Hassan, A. R. "Ultrafiltration of palm oil mill effluent: Effects of operational pressure and stirring speed on performance and membranes fouling", Environmental Engineering Research, 24(2), pp. 263–270, 2019. https://doi.org/10.4491/eer.2018.175

[43] Nair, R. R., Protasova, E., Strand, S., Bilstad, T. "Implementation of Spiegler–Kedem and Steric Hindrance Pore Models for Analyzing Nanofiltration Membrane Performance for Smart Water Production", Membranes, 8(3), Article number: 78, 2018. https://doi.org/10.3390/membranes8030078

[44] Hassan, A. R., Abdul Munaim, M. S. "Fabrication and characterization of integrally skinned-oriented highly selective charged asymmetric low pressure poly (ether sulfone) membranes for nanofiltration", Journal of Chemical Technology and Biotechnology, 87(4), pp. 559–569, 2012. https://doi.org/10.1002/jctb.2751

[45] Otero-Fernández, A., Otero, J. A., Maroto, A., Carmona, J., Palacio, L., Prádanos, P., Hernández, A. "Concentration-polarization in nanofiltration of low concentration Cr (VI) aqueous solutions. Effect of operative conditions on retention", Journal of Cleaner Production, 150, pp. 243–252, 2017. https://doi.org/10.1016/j.jclepro.2017.03.014

[46] Montesdeoca, V. A., Janssen, A. E. M., Boom, R. M., Van der Padt, A. "Fine ultrafiltration of concentrated oligosaccharide solutions–Hydration and pore size distribution effects", Journal of Membrane Science, 580, pp. 161–176, 2019. https://doi.org/10.1016/j.memsci.2019.03.019

[47] Agarwal, C., Goswami, A. "Nernst Planck approach based on non-steady state flux for transport in a Donnan dialysis process", Journal of Membrane Science, 507, pp. 119–125, 2016. https://doi.org/10.1016/j.memsci.2016.02.021

[48] Ryzhkov, I. I., Minakov, A. V. "Theoretical study of electrolyte transport in nanofiltration membranes with constant surface potential/charge density", Journal of Membrane Science, 520, pp. 515–528, 2016. https://doi.org/10.1016/j.memsci.2016.08.004

[49] Wallace, E., Cuhorka, J., Mikulášek, P. "Characterization of nanofiltration membrane and its practical use for separation of zinc from wastewater", Waste Forum, 3, pp. 314–325, 2018.

[50] Takeuchi, K., Takizawa, Y., Kitazawa, H., Fujii, M., Hosaka, K., Ortiz-Medina, J., Endo, M. "Salt rejection behavior of carbon nanotube-polyamide nanocomposite reverse osmosis membranes in several salt solutions", Desalination, 443, pp. 165–171, 2018. https://doi.org/10.1016/j.desal.2018.04.021

[51] Lebedev, D. V., Solodovnichenko, V. S., Simunin, M. M., Ryzhkov, I. I. "Effect of Electric Field on Ion Transport in Nanoporous Membranes with Conductive Surface", Petroleum Chemistry, 58(6), pp. 474–481, 2018. https://doi.org/10.1134/S0965544118060075

[52] Robinson, S., Abdullah, S. Z., Bérubé, P., Le-Clech, P. "Ageing of membranes for water treatment: Linking changes to performance", Journal of Membrane Science, 503, pp. 177–187, 2016. https://doi.org/10.1016/j.memsci.2015.12.033

[53] Schirg, P., Widmer, F. "Characterisation of nanofiltration membranes for the separation of aqueous dye-salt solutions", Desalination, 89(1), pp. 89–107, 1992. https://doi.org/10.1016/0011-9164(92)80154-2

[54] Bowen, W. R., Welfoot, J. S. "Modelling of membrane nanofiltration-pore size distribution effects", Chemical Engineering Science, 57(8), pp. 1393–1407, 2002. https://doi.org/10.1016/S0009-2509(01)00412-2

[55] Bowen, W. R., Mohammad, A. W. "Characterization and Prediction of Nanofiltration Membrane Performance—A General Assessment", Chemical Engineering Research and Design, 76(8), pp. 885–893, 1998. https://doi.org/10.1205/026387698525685

[56] Pesek, S. C., Koros, W. J. "Aqueous quenched asymmetric polysulfone hollow fibers prepared by dry/wet phase separation", Journal of Membrane Science, 88(1), pp. 1–19, 1994. https://doi.org/10.1016/0376-7388(93)E0150-I

[57] Agboola, O., Maree, J., Kolesnikov, A., Mbaya, R., Sadiku, R. "Theoretical performance of nanofiltration membranes for wastewater treatment", Environmental Chemistry Letters, 13(1), pp. 37–47, 2015. https://doi.org/10.1007/s10311-014-0486-y

[58] Roy, Y., Warsinger, D. M., Lienhard, J. H. "Effect of temperature on ion transport in nanofiltration membranes: Diffusion, convection and electromigration", Desalination, 420, pp. 241–257, 2017. https://doi.org/10.1016/j.desal.2017.07.020

[59] Garcia-Ivars, J., Iborra-Clar, M.-I., Alcaina-Miranda, M.-I., Van der Bruggen, B. "Comparison between hydrophilic and hydrophobic metal nanoparticles on the phase separation phenomena during formation of asymmetric polyethersulphone membranes", Journal of Membrane Science, 493, pp. 709–722, 2015. https://doi.org/10.1016/j.memsci.2015.07.009

[60] Hassan, A. R., Rozali, S., Safari, N. H. M., Besar, B. H. "The roles of polyethersulfone and polyethylene glycol additive on nanofiltration of dyes and membrane morphologies", Environmental Engineering Research, 23(3), pp. 316–322, 2018. https://doi.org/10.4491/eer.2018.023

[61] Safari, N. H. M., Hassan, A. R., Takwa, C. W. I. C. W., Rozali, S. "Deduction of Surfactants Effect on Performance, Morphology, Thermal and Molecular Properties of Polymeric Polyvinylidene Fluoride (PVDF) Based Ultrafiltration Membrane", Periodica Polytechnica Chemical Engineering, 63(1), pp. 27–35, 2019. https://doi.org/10.3311/PPch.12423

[62] Cohen-Tanugi, D., Grossman, J. C. "Nanoporous graphene as a reverse osmosis membrane: Recent insights from theory and simulation", Desalination, 366, pp. 59–70, 2015. https://doi.org/10.1016/j.desal.2014.12.046

[63] Liu, G., Ye, H., Li, A., Zhu, C., Jiang, H., Liu, Y., Han, K., Zhou, Y. "Graphene oxide for high-efficiency separation membranes: Role of electrostatic interactions", Carbon, 110, pp. 56–61, 2016. https://doi.org/10.1016/j.carbon.2016.09.005

[64] Kamcev, J., Galizia, M., Benedetti, F. M., Jang, E.-S., Paul, D. R., Freeman, B. D., Manning, G. S. "Partitioning of mobile ions between ion exchange polymers and aqueous salt solutions: importance of counter-ion condensation", Physical Chemistry Chemical Physics, 18(8), pp. 6021–6031, 2016. https://doi.org/10.1039/C5CP06747B

[65] Ismail, A. F., Hassan, A. R., Cheer, N. B. "Effect of shear rate on the performance of nanofiltration membrane for water desalination", Songklanakarin Journal of Science Technology, 24(Suppl.), pp. 879–889, 2002. [online] Available at: http://rdo.psu.ac.th/sjstweb/journal/24-Suppl-1/14nanofiltration-membrane.pdf [Accessed: 07 April 2021]